Fifth-Generation Low-Density Parity-Check Codes in the Turbo Equalization of Faster-than-Nyquist Signaling

Asma A. Alqudah[1*], Khaled F. Hayajneh[2], Hasan A. Aldiabat[1], and Hazim M. Shakhatreh[1]

[1]Department of Telecommunications Engineering, Hijjawi Faculty for Engineering Technology, Yarmouk University, Irbid 21163, Jordan.

[2]Computer Engineering Department, College of Engineering and Technology, American University of the Middle East, Egaila 54200, Kuwait

Email: asma.qudah@yu.edu.jo (A. A. A.); Khaled.hayajneh@aum.edu.kw (K. F. H.); hasan.aldiabat@yu.edu.jo (H. A. A.); hazim.s@yu.edu.jo (H. M. S.)

*Corresponding author

***Abstract*—The so-called faster-than-Nyquist signaling scheme has recently emerged as a highly promising technique, garnering significant attention for its remarkable ability to efficiently utilize bandwidth by packing more data than conventional systems. In parallel, employing Low-Density Parity-Check (LDPC) codes, a celebrated capacity-approaching forward-error correction (FEC) technique has revolutionized communications. This paper investigates the performance of the 5G new radio layered LDPC codes when employed as the constituent outer block for decoding within the context of the iterative turbo equalization method. The focus lies on effectively mitigating the severe interference introduced by the faster-than-Nyquist (FTN) scheme. The LDPC coding is implemented using parity check matrices derived from the 5G communications standard. To evaluate the system's performance, simulations are conducted using varying sizes of base matrices. Simulations demonstrate the impact of employing different base matrix sizes and quantify the performance gain achieved by employing varying numbers of iterations for the decoding process. The obtained results showcase the superiority of the proposed scheme, as measured by the signal-to-noise ratio (SNR) gain (in dB) when compared to a Nyquist signaling system possessing the same data-carrying capabilities. These findings offer compelling evidence of the potential of our proposed approach in terms of enhancing spectral efficiency and delivering improved performance in the presence of severe interference. The approach utilizes the regularity in the structure of the 5G NR LDPC base matrices and provides efficient layered decoding scheme that contributes to the fast convergence of the decoding process. The proposed scheme of the 5G NR LDPC decoder in the context of severe FTN turbo equalization proves superior to the uncoded QPSK transmission over additive white Gaussian noise (AWGN) channel, with a gain of ~5 dB at the same data rate and the same transmission power.**

***Keywords*—5G low-density parity check, faster-than-Nyquist, belief propagation, iterative decoding, log-likelihood ratio, intersymbol interference, turbo equalization**

Manuscript received August 2, 2024; revised September 4, 2024, accepted September 13, 2024; published November 25, 2024.

I. Introduction

The field of mobile telephony has undergone remarkable growth, with non-voice-based services surpassing voice-based usage. As mobile phones have evolved beyond simple voice communications, the need for broadband communications to support wireless technology advancements has become essential. To meet this demand, one favorable approach involves modifying the existing systems' bandwidth allocation. Faster-than-Nyquist (FTN) signaling is an example of such an approach, prioritizing increased processing complexity in exchange for bandwidth utilization.

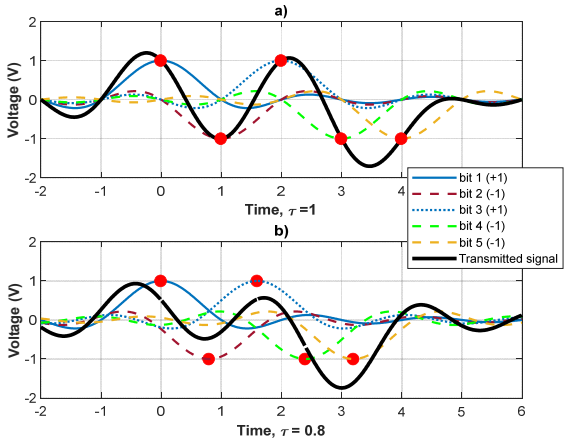

Fig. 1. Illustration of FTN signalling where a) T=1, τ=1, Nyquist and b) T=1, τ=0.8, FTN. The factor τ represents the compression in time.

In today's context, bandwidth has become a limited resource compared to the processing capabilities offered by advanced semiconductor technology. Therefore, exploring approaches like FTN, which prioritize efficient bandwidth utilization by trading processing complexity, is crucial.

In 1962, Gallager first proposed low-density parity-check (LDPC) codes [1]. In 1996, McKay and Neal [2] revised the LDPC codes and found that irregular LDPC performed better than regular LDPC [3, 4]. Irregular

LDPC codes can operate close to the Shannon limit for error performance. Ulkarni and Sankar [5] proposed an efficient technique to get irregular LDPC codes from regular ones. The concept of faster-than-Nyquist signaling was first introduced by J. Mazo in 1975 [6]. The adoption challenges faced by LDPC codes, which were introduced in 1962 but not widely utilized until the early 2000s, mirror the complexity associated with the transceivers used in FTN signaling [1]. FTN involves transmitting signals at rates higher than the Nyquist rate typically required for interference-free transmission [7–9]. By raising the data transmission rate while maintaining a constant power spectral density (PSD), FTN achieves enhanced bandwidth efficiency. Intentional intersymbol interference (ISI) is introduced in FTN by allowing consecutive symbols carrying information to overlap in time.

The non-orthogonal transmission scheme of FTN holds significant promise for wireless communications as it inherently enhances spectrum efficiency by increasing the data rate. In today's bandwidth-constrained environment, FTN has attracted attention due to its ability to transmit 30%–100% more data within equivalent bandwidth, bit energy, and error rates compared to conventional orthogonal transmission systems. Fig. 1 illustrates an instance of FTN pulse shaping using sinc pulses, where the symbol time is T=1. In the first part a) of the figure, conventional orthogonal linear modulation is employed with the pulse shape defined as $h(t) = \sqrt{\frac{T}{\pi t}}\sin(\frac{\pi t}{T})$, using τ=1 with the lighter sinc pulses in this part corresponding to the symbols +1, -1, +1, -1, -1 which sum up to create the denser, heavier curve representing the transmitted signal. In part b) of the same figure, FTN modulation is applied with the same symbol time T=1 but τ=0.8. Here, it can be observed that the five sinc pulses are temporally advanced by increments of 0, 0.2, 0.4, and so on. By examining Fig. 1, it becomes evident that at τ=0.8, $1/\tau$ =1.25, which means that 25% more bits can be transmitted within the same bandwidth without a detrimental impact on the error rate.

Subsequent studies have explored the use of a raised cosine (RC) pulse instead of a sinc pulse in FTN signaling, as well as the impact of varying roll-off factors on the Mazo threshold [10]. Researchers have also sought to mitigate the significant ISI introduced by FTN through the use of a trellis-based equalizer at the receiver. While joint equalization and decoding would be the optimal approach for minimizing bit-error-rate (BER) and accurately detecting transmitted data, the exponentially growing complexity of this method with increasing data length has prompted the pursuit of alternative options [11]. Turbo equalization, involving iterative equalization and decoding of FTN ISI channels, has emerged as a highly promising detection method [12–14].

This research paper focuses on the utilization of turbo equalization in a serial concatenation setup, where the equalizer compensates for the effects of the ISI channel before applying a standard decoding algorithm for error control code (ECC). Within the context of turbo equalization, the equalizer (inner decoder) and the decoder (outer decoder) exchange soft information in the form of log-likelihood ratios pertaining to the transmitted data symbols. In this study, the constituent block responsible for decoding is the 5G new radio (NR) layered LDPC code. Previous works have explored the application of FTN signaling to counteract potential rate loss in short packet communications by combining a low-complexity FTN signaling detector with nonbinary LDPC (NB-LDPC) codes [15]. Therein, this paper employs the NB-LDPC coding in the context of FTN signaling with low complexity FTN detector (successive symbol-by-symbol with go-back-K sequence estimation). The attained results show that NB-LDPC codes have advantages in the low SNR region as well as for large values of τ, i.e. for $\tau \geqslant 0.8$. In addition, this paper suggests that for light ISI scenarios, it is sufficient to use a low-complexity FTN signaling detector with NB-LDPC rather than using a complex FTN signaling detector with LDPC. Optimization methods for LDPC convolutional codes in FTN systems have also been investigated, focusing on obtaining favorable degree distributions and girth. Comparative analyses have shown significant gains when compared to LDPC block codes specified in standards like worldwide interoperability for microwave access (WiMAX) [16]. Furthermore, the authors in [17] have proposed an approach to designing unstructured parity-check matrices for FTN signaling. The design is based on optimizing the code performance using extrinsic information transfer (EXIT) charts. The achieved results outperformed the classical LDPC codes optimized for AWGN channels.

When it comes to the potential real-world scenarios of the proposed approach in this study, it is worth noting that LDPC coding schemes and turbo equalization techniques present methods used in digital communication systems to improve the efficiency and reliability of data transmission. When integrated with FTN signaling, these methods can have significant implications in various real-world applications, particularly in the context of 5G technology. To mention some, autonomous vehicles, industrial automation, and remote healthcare require reliable, high-speed, and low-latency data transmission in order to ensure that critical information reaches its destination accurately and swiftly. These requirements can be achieved as a direct consequence of utilizing LDPC codes and turbo equalization in conjunction with FTN signaling.

What is unique about our approach is that it employs the 5G NR LDPC codes in the context of FTN signaling to test how well the 5G codes perform when applied with the promising bandwidth-efficient FTN scheme. The special thing about using the 5G NR LDPC codes is that these standard codes have a structured configuration where they can be expanded uniformly and systematically to match several hundreds of block lengths. Furthermore, the uniform structure of the 5G NR LDPC base graphs allows the designer to achieve customized code rates by applying message-bit and parity-bit puncturing. The ability to realize puncturing is backed by the fact that the 5G NR LDPC base graphs have the unique structure of a fixed and standard form, and the existence of the double-diagonal portion in the graphs helps with the achievement of particular code rates for the 5G NR LDPC codes. Once

more, the standard form of the 5G NR LDPC codes allows additionally the efficient and straightforward application of the layered decoding of FTN signals at the turbo receiver. This feature is not available for other sparse-graph based codes or unstructured classical LDPC codes.

The structure of this paper is as follows: Section II presents the literature review and Section III describes the FTN signaling system. Section IV elaborates on the 5G NR LDPC codes and their decoders while Section V analyzes the LDPC-coded faster-than-Nyquist system. In Section VI, simulation results are presented and in Section VII the system complexity is described. Section VIII draws conclusions based on the findings, and finally, some future work directions are mentioned in Section IX.

II. Literature Review

In this section, we present an overview of selected research articles regarding LDPC codes and combined system applications of both LDPC and FTN scenarios.

A. 5G LDPC Coding Overview

Jayawickrama, Abewardana *et al.* [18] propose improvements to the well-known layered normalized min-sum algorithm for 5G NR LDPC. They develop an improved 5G decoding algorithm utilizing the existing bit structure of the 5G transport blocks. They then use a deep neural network to determine the optimal normalization factors for the proposed algorithm. Simulation results demonstrate an enhancement of 0.3–1.9 dB at no additional cost for hardware multiplier resources. Therefore, the proposed algorithm is efficient for the practical implementation of 5G decoders.

Roberts, Michaelraj *et al.* [19] provide a comprehensive overview of the basic concepts and performance analysis of LDPC decoding. They briefly describe the general classification and computational complexity evaluation of existing soft decision-based decoding methods. From this research work, they conclude that convergence speed, hardware complexity, decoding stability, and computational overhead still need more experimental evaluation and research. To overcome these challenges, many leading researchers have proposed important decoding methods that use LDPC codes. Many of these available techniques have proven effective in achieving better decoding reliability while minimizing complexity. This comprehensive study shows that existing design techniques can be combined with various methodologies, such as optimization, to improve the overall performance. The authors present several unexplored issues in LDPC decoding, such as convergence speed, numerical instability, and magnitude overestimation. These issues can be exploited through experimental evaluations and detailed studies, which will be practical for many advanced wireless communication systems and their applications.

In [20], an algorithm called multi-layer progressive tree-structured edge growth is proposed to create length-scalable, rate-compatible quasi-cyclic LDPC codes with nested lifting and nested base matrices, such as 5G NR LDPC codes. This research work mainly investigates the design of nested lifting. To easily and efficiently manage the complex performance dependencies of lifting sizes and nested base matrices, a nested lifting design is decomposed into a lifting design for each lifting size, called a layer. The nested base matrix of each layer is found using a progressive tree-structured edge-growing algorithm in which a tree structure is used to store different intermediate results and to better check the performance of the error layer between the nested base matrices. Criteria consisting of performance evaluation are employed for tree pruning, minimum distance verification, and improved cycle classification, which allows for the optimization of the performance within an acceptable complexity.

Roberts, Kingston, and Anguraj [21] present a survey research work summarizing the current advancements in LDPC decoding algorithms. Decoding algorithms are grouped and classified according to the context of their error-correcting performance, higher citation count, decoding framework, and other key features. To evaluate in detail, the characteristics of these popular hard-decision and soft-decision decoding approaches, a systematic review was conducted to determine their applicability to various open research problems. Based on this research work, it is very interesting to see how hard decision-based decoding schemes have been utilized as a successful way to solve many real-world problems. On the other hand, the alternating direction method of multipliers-based decoding approach for LDPC codes using linear programming has shown effectiveness and popularity in solving a wide range of data transmission problems with its simple but powerful decoding structure. This research work makes it clear that service providers and next-generation communication systems will need advanced and robust decoding schemes to ensure reliable communications. Therefore, developing a computationally efficient and versatile decoding scheme using LDPC codes that provide sufficient robustness for both variable and fixed channel conditions is essential. Hence, future research and development processes on LDPC decoding algorithms should evaluate the use of different methods based on parameter estimation, linear programming, and optimization to stimulate promising and new solutions.

B. LDPC in the Context of PR Channels

Khittiwitchayakul, Phakphisut and Supnithi [22] suggest altering the turbo equalization process by implementing a sliding window approach for both the spatially coupled LDPC decoder and the Bahl-Cocke-Jelinek-Raviv (BCJR) detector. The outcomes indicate that employing these modified turbo equalization schemes in the partial response (PR) channel yields improved BER performances compared to traditional turbo equalization methods. Additionally, [23] explores iterative detection and decoding for nonbinary-LDPC coded (PR) channels where these channels involve the presence of a quantizer to discretize the continuous received signal. The proposed turbo equalizer utilizes pre-computed quantized channel transition probabilities within the symbol-level BCJR channel detection

algorithm. This approach significantly reduces computational complexity by eliminating real-time floating-point multiplications. Simulation results demonstrate that, with a limited number of quantization bits, the proposed receiver closely approaches the performance of the conventional turbo equalizer operating on unquantized signals.

Moreover, Cuc, Lucian *et al.* [24] introduce an iterative framework for equalization and decoding designed to address intersymbol interference in the presence of an AWGN channel. Following the conventional turbo equalization approach, their proposed system incorporates LDPC coding at the transmitter and implements a Log maximum a posteriori probability (Log-MAP) equalizer and min-sum LDPC decoding. From their examined findings, it can be inferred that the effectiveness of equalization relies on both the channel's impulse responses and the selected decoding and equalization approach. Consequently, the equalization method may not consistently yield favorable outcomes for every channel scenario.

III. System Description

We consider the overall communications system presented in Fig. 2. It can be seen as a bit-interleaved coded modulation scheme composed of a channel code serially concatenated with a binary linear modulation pulse-shaped using FTN signaling.

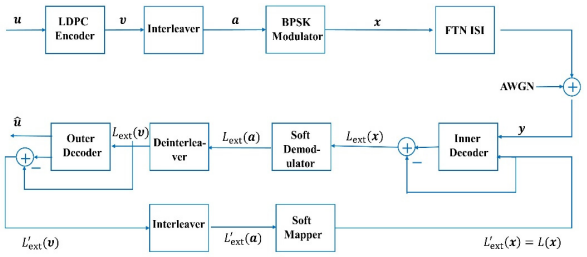

Fig. 2. FTN turbo equalization receiver employing an LDPC decoder.

The baseband form of the ordinary linearly modulated signals is [11]

$$s_x(t) = \sum_0^\infty x_n h(t - n\tau T), \quad \tau \le 1 \tag{1}$$

where x_n are real equiprobable independent and identically distributed binary data symbols, and h(t) is a T-orthogonal baseband pulse. In Eq. (1), when $\tau = 1$ this underlies the Nyquist signaling, while when $\tau < 1$, this is FTN signaling. The variable τ is called the packing factor of the system.

The interesting thing about FTN is that even when the symbols are sent faster, the minimum Euclidean distance of the signal set remains unchanged, up to a certain limit [6]. Hence, the asymptotic error rate behavior of an optimal decoder remains unchanged. In addition, FTN works by reducing the time spacing between adjacent pulses below the Nyquist rate while keeping a fixed power-spectral density.

The FTN signal, when τ<1, in Eq. (1) is transmitted over an AWGN channel $\sim \mathcal{N}_c(0, \sigma^2)$. The equivalent discrete-time representation of the received signal is

$$\mathbf{y} = \mathbf{x} * \mathbf{f} + \boldsymbol{\eta} \tag{2}$$

where η is a random Gaussian sequence with zero mean and autocorrelation $\phi_\eta(j, j+n) = N_0\delta[n]$, $\mathbf{x}$ is the transmitted data symbols, and f is the FTN channel coefficients.

In this paper, we adopt the typical super minimum phase model **f**, presented in [25], for the 30% root raised cosine (rRC) FTN pulse stretched in time by τ=0.5. This value of the stretching factor is based on a prior work presented in [25]. The unit-energy model is

$$\begin{aligned}\mathbf{f} = [&-0.005, -0.003, 0.007, -0.011, -0.001, 0.034,\\ &-0.019,\ 0.003, \mathbf{0.375}, \mathbf{0.741}, \mathbf{0.499}, \mathbf{-0.070},\\ &\mathbf{-0.214}, \mathbf{0.019}, \mathbf{0.087}, \mathbf{-0.020}, \mathbf{-0.028},\\ &\mathbf{0.017}], \tau = 0.5.\end{aligned} \tag{3}$$

As the precursor values are written in lightface in Eq. (3); all detectors replace these with zeros and work at a delay K_p. The τ=0.5 represents a 50% bandwidth reduction of the system. Additional material on FTN can be found in [26–30].

Since FTN introduces intentional ISI in the transmitted signal with a memory-L channel response, then the receiver design is more complex than the simple symbol-by-symbol detector. As the ISI in the received FTN signal is trellis-structured, then a maximum-likelihood sequence estimation/maximum a posteriori (MLSE/MAP)-based detector is required.

Fig. 2 shows the nearly-optimal iterative receiver structure implemented in this work for the turbo equalization of the FTN signals in Eq. (2). In the figure, L_{ext} denotes the extrinsic log-likelihood ratios (LLRs). The LLRs are defined later in Eq. (6). The structure shown in Fig. 2 comprises of two component decoders that handle soft-input and soft-output. The inner decoder, known as the equalizer, is responsible for ISI decoding. To mitigate errors between adjacent symbols in a data block, an interleaver and a deinterleaver are incorporated into the iterative process. Both turbo decoders share the data sequence **x**, which serves as the input for the inner decoder and is also shuffled at the output of the outer decoder. The main objective of the iterative process is to reach to an agreement between the two decoders regarding the final decision on $\hat{\boldsymbol{x}}$, rather than $\hat{\boldsymbol{u}}$. The receiver's BER performance is significantly enhanced by exchanging soft information between the component decoders instead of relying solely on hard-decision symbols. However, this improvement in performance comes at the cost of increased receiver complexity. Moreover, since the iterative detection needs to be performed for each data block multiple times, the receiver's complexity is further amplified. This research paper employs 5G NR LDPC codes for the outer decoder, while the intentional ISI, introduced by the FTN signaling, functions as the inner encoder.

In the existing literature, various options are available for the soft-input soft-output (SISO) equalizer. However, in this study, the chosen equalizer is the MAP-based BCJR algorithm. It is important to highlight that in this configuration, the outer decoder is responsible for decoding a probabilistic channel to generate the ultimate output $\hat{\boldsymbol{u}}$.

The MAP decoder is a key component in decoding LDPC codes, and it represents the most computationally intensive part of LDPC decoding, especially for codes with large block lengths and high code rates. The complexity of the MAP decoder grows exponentially with the number of bits in the code block, making it the primary bottleneck in LDPC decoding systems. The main goal of LDPC decoding is to accurately estimate the transmitted codeword despite the presence of channel noise and other impairments. This goal is achieved by iteratively updating the probabilities associated with each received bit. The updating operation is based on the received signal as well as a probabilistic model of the channel, and it continues until it reaches a point where there is no further significant change or improvement, indicating that convergence has been achieved.

Within Fig. 2, the equalizer performs computations for the a posteriori probabilities (APPs) $\Pr(x_n = x|\boldsymbol{r})$ at each depth n, where x belongs to the set of modulation alphabets $\boldsymbol{\Omega}$ and r represents the received sequence. The extrinsic log-likelihood ratios, denoted as $L_{\text{ext}}(\boldsymbol{x})$, are derived by subtracting the a priori LLRs, $L(\boldsymbol{x})$, from the a posteriori LLRs obtained from the equalizer. These extrinsic LLRs serve as a priori information that is transmitted to the outer decoder. This process is shown in the following equations.

$$L_{\text{apriori}}(x_n) = \log\left(\frac{\Pr(x_n=+1)}{\Pr(x_n=x)}\right), \tag{4}$$

$$L_{\text{posterior}}(x_n) = \log\left(\frac{\Pr(x_n=+1|\boldsymbol{r})}{\Pr(x_n=x|\boldsymbol{r})}\right), \tag{5}$$

$$L_{\text{ext}}(x_n) \triangleq L_{\text{posterior}}(x_n) - L_{\text{intrinsic}}(x_n),\ x \in \Omega \tag{6}$$

The outer decoder supplies the a priori information in this context. At the initial iteration, as no a priori information is present, it is assumed that that $L(x_n) = 0, \forall\, n$. The assumption of independence among data symbols is considered, which is supported by the use of interleavers and large block sizes [25]. These assumptions, coupled with the treatment of extrinsic information as a priori, are two fundamental traits of any turbo receiver. Extrinsic information, in the probabilistic domain, refers to the generated information regarding a specific symbol x_n considering only the information from other symbols $x_l,\ l \neq n$.

Moving on to the outer decoder, it computes the APPs $\Pr(v_n = x|L(\boldsymbol{v}))$ at each depth n. These calculations are based solely on the a priori LLRs denoted as $(\boldsymbol{v}) = \Pi^{-1}(L_{\text{ext}}(\boldsymbol{x}))$. The extrinsic LLRs are obtained by subtracting the a priori LLRs, and this process is represented by Eq. (6).

IV. Low-Density Parity Check Codes in the 5G NR Standard

Low-density parity check codes are a class of linear block codes that are characterized by a sparse $(N-K) \times N$ parity check matrix $\boldsymbol{H}$. The LDPC code is always associated with the parity-check matrix, which can be represented using a bipartite graph of checks and nodes called the Tanner graph, as shown in Fig. 3. For a binary LDPC code, the parity-check matrix has a small number of '1' entries compared to '0' entries, making it sparse and allowing the encoder computational complexity to be reduced.

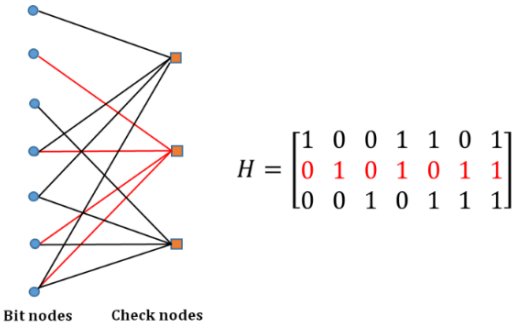

Fig. 3. Graphical representation of a parity-check matrix using Tanner graph.

For a K-bit message sequence and an N-bit codeword C, the Tanner graph consists of N message nodes (on the left) and $(N-K)$ check nodes (on the right); see Fig. 3.

The codewords of the LDPC code are those length-N vectors such that for all check nodes, the sum of the code bits connected to each check node is zero. Mathematically, this is represented as

$$\boldsymbol{H}.\boldsymbol{C}^{\boldsymbol{T}} = \boldsymbol{0}, \tag{7}$$

and the sparsity of the $\boldsymbol{H}$-matrix is critical to efficiently implementing the decoding algorithm.

LDPC encoding is performed in a similar way as in linear block codes. In the 5G NR LDPC coding the 5G parity-check matrix $\boldsymbol{H}$ and the given data sequence are used to generate the codewords, since the codewords are generated systematically. Each LDPC code vector in the 5G standard is represented systematically as $\boldsymbol{C} = [\boldsymbol{m_1}, \boldsymbol{m_2}, \boldsymbol{m_3}, \ldots, \boldsymbol{m_K}, \boldsymbol{p_1}, \boldsymbol{p_2}, \boldsymbol{p_3}, \ldots, \boldsymbol{p_{N-K}}]$, where $\boldsymbol{m_i}$ is a message bit and $\boldsymbol{p_i}$ is a parity bit. The 5G parity-check matrices are generated systematically as well, where the H matrix is represented in the following standard form

$$\boldsymbol{H} = [\boldsymbol{P}\ \boldsymbol{I}] \tag{8}$$

where $\boldsymbol{P}$ is an $(\boldsymbol{N}-\boldsymbol{K}) \times \boldsymbol{K}$ parity block and $\mathbf{I}$ is $(\boldsymbol{N}-\boldsymbol{K}) \times (\boldsymbol{N}-\boldsymbol{K})$ identity block matrix. Therefore, using the syndrome condition in Eq. (7), all the parity bits can be evaluated straightforwardly.

A. LDPC Decoding

LDPC decoders are based on a general class of decoders called message-passing decoders, which are iterative. The name is because of the nature of the LDPC decoder, where messages are passed between message nodes and check nodes in iterative loops.

The belief propagation (BP) algorithm is a crucial subclass of message-passing algorithms. In BP, messages in the form of beliefs are interchanged between the message and check nodes. These beliefs are represented in the form of LLRs. The LLRs that move back and forth between the message and check nodes are extrinsic LLRs. The process of exchanging the LLRs is called soft decoding.

The soft decoding process of LDPC codes consists of two main steps. The first step is called the vertical step, in which the check nodes update their soft information. The second step is the horizontal one, in which the message nodes update their soft information.

The soft information generated at both the check and message nodes are represented using LLRs. The LLRs at the check nodes are passed to the message nodes, and the LLRs generated at the message nodes are passed back to the checks.

For each nonzero entry in the parity-check matrix, let's define $\boldsymbol{\eta_{m,n}}$ as the LLR message sent from check node $\boldsymbol{m}$ to bit node $\boldsymbol{n}$.

$$\boldsymbol{\eta_{m,n}} = -\mathbf{2}\tanh^{-1}\left(\prod_{j\in N_{m,n}}\tanh\left(-\frac{\lambda_j-\eta_{m,j}}{2}\right)\right) \quad (9)$$

where $\boldsymbol{N_{m,n}}$ means the positions in the $\boldsymbol{m}^{\mathbf{th}}$ row in $\mathbf{H}$ except the one in the $\boldsymbol{n}^{\mathbf{th}}$ column. In addition, let's define $\boldsymbol{\lambda_n}$ as the LLR of the bit node $\boldsymbol{n}$, then

$$\boldsymbol{\lambda(C_n\backslash L(v)) = L_c v_n + \sum_{m\in M_n}\eta_{m,n}} \quad (10)$$

where $\boldsymbol{L_c}$ is the channel reliability and $\boldsymbol{v_n}$ is the n$^{\text{th}}$ received de-interleaved symbol from the inner equalizer.

The value $\boldsymbol{\lambda(C_n\backslash L(v))}$ represents the total belief the decoder assumes about bit node $\boldsymbol{C_n}$, given the received sequence $\boldsymbol{v}$. If we are employing an iterative decoder, alternating between Eq. (9) and Eq. (10), then we need to remove from $\boldsymbol{\lambda(C_n\backslash L(v))}$ the message that it has already received from that check node $\boldsymbol{\eta_{m,n}}$. This represents the extrinsic information passed by the decoder, see Fig. 4.

When the LDPC decoder finishes its internal iterations, it sends back its extrinsic LLR $\boldsymbol{\lambda}$ to the inner FTN BCJR equalizer as a priori information. The inner equalizer then performs a new outer iteration as in Eq. (6), and so on. Using the above iterative decoder, when the decoder reaches the last iteration, Eq. (10) is used to make decisions about the bit code, and the loop terminates.

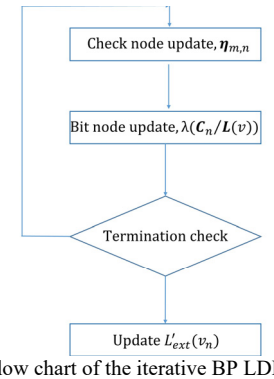

Fig. 4. A flow chart of the iterative BP LDPC decoder.

B. LDPC Base Matrices in the 5G New Radio Standard

Using a base graph and expansion method, the 5G NR standard specifies parity check matrices for LDPC [31]. There are two main base graphs and several possible expansion factors. The two base matrices in the 5G NR standard are base graph 1 (BG1) of dimension 46×68 and the other is base graph 2 (BG2) of dimension 42×52. A new base matrix is formed for each base graph and expansion factor. Therefore, there are plenty of possible base matrices. Fig. 5 shows a typical example of a base matrix generated from BG2 along with an expansion factor of z=64.

Fig. 5. A base matrix from BG2 and an expansion factor of 64.

The code rate for BG1 is

$$\boldsymbol{R = \frac{K}{N} = \frac{68-46}{68} = \frac{22}{68}} \quad (11)$$

where K represents the number of message bits and N the number of coded bits. For BG2, the code rate is

$$\boldsymbol{R = \frac{K}{N} = \frac{52-42}{52} = \frac{10}{52}} \quad (12)$$

As the code rate for BG2 is less than the code rate for BG1, we expect to have better performance when employing BG2 in generating the parity-check matrix; since BG2 involves more redundancy than BG1.

V. Receiver Iteration of LDPC-Coded Faster-Than-Nyquist Signaling

5G NR LDPC codes possess several distinguishing characteristics that set them apart from other coding schemes since these codes often use protograph-based designs, which provide an efficient graphical representation for code optimization and allow for easier encoding and decoding. Additionally, 5G NR LDPC decoding often employs a layered approach, where nodes are processed in layers, starting with the most reliable ones. This approach can lead to faster convergence and lower latency.

In the serially concatenated system of FTN equalizer followed by an LDPC decoder, the LLRs are not only exchanged between the check and message nodes within the LDPC decoder; but additionally, the LLRs are exchanged between the FTN equalizer and the LDPC decoder as well.

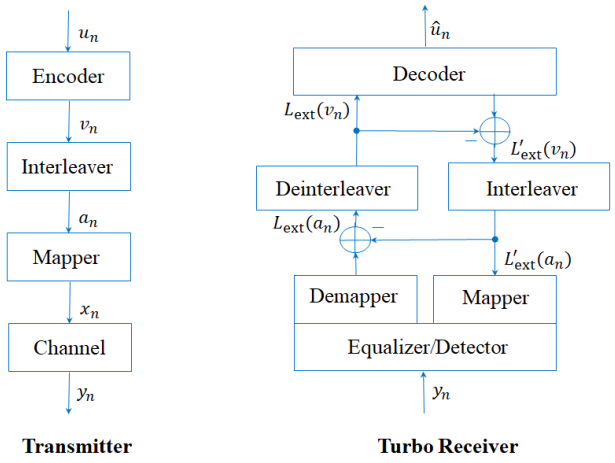

Fig. 6. System configuration and turbo equalization.

The inner equalizer calculates its beliefs about each code bit and then sends these beliefs to the outer LDPC decoder. In the same manner, the LDPC decoder calculates other likelihood quantities and sends them back to the inner equalizer. This process proceeds iteratively until a certain condition is met. See Fig. 6.

The extrinsic LLRs in Eq. (6), $\boldsymbol{L_{ext}}$, are sent to the LDPC decoder as a priori information. They are used at the decoder to update the bit nodes, and then the internal LDPC iterative loop starts. It proceeds back and forth between the check and bit nodes for a prescribed number of loops. When the LDPC decoder iterations stop, the extrinsic LLRs in Eq. (10) are sent back to the FTN equalizer as a priori information, and so on.

VI. Results

The simulation setup applies FTN turbo equalization and a rate (K, N) LDPC code combined with binary modulation. The simulations run for 10 outer iterations. It is important to note that in the presented theoretical and simulation results, we used logarithmic representation in computing LLRs instead of directly computing them as ratios of probabilities. This is clearly demonstrated in Eqs. (4–6). It is known that upon using the logarithmic representation, small values are more accurately represented, and the effect of underflow is mitigated by converting the multiplication operations into addition operations. Additionally, while performing the BCJR algorithm at each trellis depth and while computing the forward and backward state metrics a normalization process takes place for all state probabilities. This process is described as follows:

$$\alpha(state_i \backslash x_n = +1)_{normalized} = \frac{\alpha(state_i \backslash x_n = +1)}{\sum_i \alpha(state_i \backslash x_n = +1) + \sum_i \alpha(state_i \backslash x_n = -1)} \quad (13)$$

$$\alpha(state_i \backslash x_n = -1)_{normalized} = \frac{\alpha(state_i \backslash x_n = -1)}{\sum_i \alpha(state_i \backslash x_n = +1) + \sum_i \alpha(state_i \backslash x_n = -1)} \quad (14)$$

where $\alpha(state_i \backslash x_n = +1)$ represents the forward probability for the i^{th} state, at a certain depth n in the trellis, given symbol $x_n = +1$ is transmitted. The quantity in the denominator in both Eq. (13) and Eq. (14) represents the total forward probability of all states, at a certain depth n in the trellis, for both transmitted symbols $x_n = +1$ and $x_n = -1$. The same normalization process takes place when calculating the backward recursion probabilities as well.

In our simulations, the full BCJR algorithm is not used because of the intractable trellis size that results from employing an 18-tap ISI channel. Instead, the reduced complexity M-BCJR algorithm is used in the equalizer, where only M surviving states are kept at each trellis depth, with the values of M chosen such that the system complexity converges to a small number of states at practical values of signal-to-noise ratio (SNR).

For the LDPC parameters, the decoding is carried out by dividing the parity-check matrix into layers. The soft information from one layer is used to update the check nodes of the next layer, and so on, until the whole matrix is finished. The layered approach in LDPC decoding can significantly influence the decoding process, often leading to improved performance. In the layered approach, variable and check nodes are organized into different layers, often based on their reliability. Decoding starts with the most reliable nodes in the first layer and proceeds to less reliable nodes in subsequent layers. Furthermore, it can be implemented with parallel processing, allowing multiple layers to be processed simultaneously. This parallelism can speed up decoding, making it suitable for high-throughput communication systems, and by processing layers of nodes in order of reliability, the layered approach helps control the computational complexity of the decoder. Layered LDPC decoding can also be adaptive, meaning the order and number of layers can be adjusted based on the desired code rate. The number of internal iterations within the decoder is varied, and the simulation results are recorded each time.

In all of the following simulations, the LDPC-coded binary phase shift keying (BPSK)-modulated signal sequence is sent over the AWGN channel at a faster rate than the Nyquist rate by stretching the transmission pulse by $\tau = 0.5$, which means that the data rate is doubled.

The simulations are then carried out by changing some parameter values in the serially-concatenated turbo equalizer at the receiver.

The received sequence is passed first through an FTN equalizer; then, the demodulated output is passed through a layered LDPC decoder. Finally, the equalizer and the decoder output soft information are in the form of LLRs. These LLRs go through two different kinds of loops; outer loops that involve both the equalizer and the decoder, and inner loops that happen only within the LDPC decoder. In our simulation, we test the turbo equalizer performance when employing a different number of iterations for the inner loops. Fig. 5 shows a schematic of the entire simulation chain applied in our work.

Additionally, a wide range of base matrices was generated from BG1 and BG2 using different values of expansion factors from the 5G NR standard. The FTN system was tested again using these different base matrices, and the following simulation results were attained.

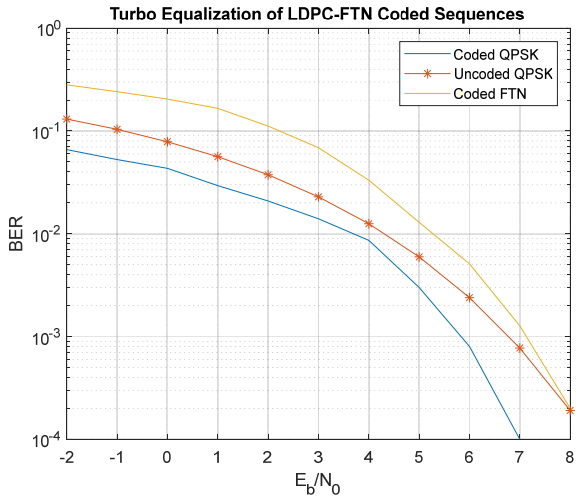

Fig. 7. BER vs E_b/N_0 (dB) for turbo equalization of coded FTN sequences with system parameters as follows: BG1 base matrix, z = 2, and number of inner iterations 1. For the LDPC-coded QPSK of the same transmission rate, the LDPC decoder applies 1 inner iteration.

In Fig. 7, the performance of FTN equalization is shown for LDPC coding using a base matrix of BG1 and an expansion factor z = 2. The number of outer turbo iterations is 10. The number of inner iterations is 1 iteration. The performance is depicted along with the BER of the uncoded quadrature phase-shift keying (QPSK) as well as LDPC-coded QPSK over the AWGN channel for comparison.

It is shown in Fig. 7 that the performance of the LDPC-coded FTN system is a bit worse than the uncoded QPSK as well as the LDPC-coded QPSK. This performance, with only 1 inner iteration, is considered pretty good for an 18-tap ISI channel. This number of 1 inner iteration is way too small to manifest the power of the LDPC coding for both systems, i.e., the FTN and QPSK LDPC-coded systems. With only 1 inner LDPC iteration, the reliability of the LLR values exchanged between the bit and check nodes is very poor. This justifies the unsatisfactory performance of the system in Fig. 7.

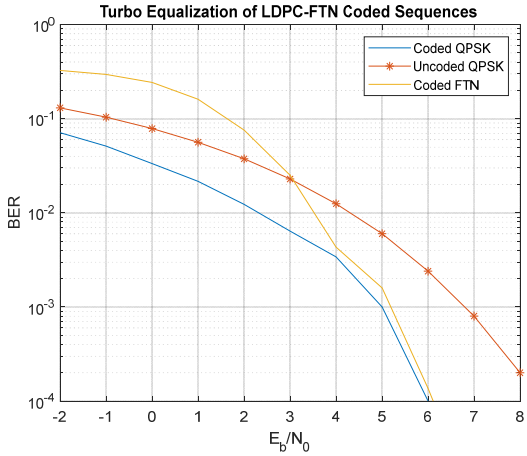

Fig. 8. BER vs E_b/N_0 (dB) for turbo equalization of coded FTN sequences with system parameters as follows: BG1 base matrix, z = 2, and number of inner iterations 6. For the LDPC-coded QPSK of the same transmission rate, the LDPC decoder applies 6 inner iterations.

If the number of inner iterations for the LDPC decoder is increased, the power of the LDPC code will start to show up. In Fig. 8, the same setup was used but with a change in the number of inner LDPC iterations to 6. It is noticed in Fig. 8 that the performance has improved as we increased the number of inner iterations. An amount of ~2 dB of signal-to-noise ratio has been saved in the waterfall region in the FTN curve when going from 1 to 6 inner iterations. This reduced amount of SNR translates into an improved error performance of the system at the same power consumption as compared to equivalent systems or it means less power consumption, i.e. by $\sim\frac{1}{2}$, of the system to achieve a required error performance. The slight performance improvement is due to the fact that a small value of the expansion factor z has been used in the parity-check matrix. A smaller z means a denser parity check matrix. The denser the parity-check matrix, the less improvement is achieved because of the need to employ more iterations at the receiver. Nevertheless, we notice an improvement in the quality of decoded data with the increase of inner LDPC iterations. Additionally, it is notice from the same figure that the performance of BPSK LDPC-coded FTN approaches the same performance as the LDPC-coded QPSK system except for the low SNR region where the latter outperforms the former by an amount of ~3 dB.

It is essential to mention here that in our work, the maximum value of inner iterations used in our simulations is 6; since we have yet to notice any significant improvement in performance when going beyond 6 iterations.

In Fig. 9, the performance of turbo equalization for the same system setup is shown but with changing the expansion factor of the base matrix to 32. In the same figure, six curves are portrayed; two are for BPSK LDPC-coded FTN with a different number of inner iterations, two for LDPC-coded QPSK with a different number of inner iterations as well, one for the turbo

equalizer BPSK but employing a convolutional encoder as the outer constituent decoder, and the last one is uncoded QPSK over AWGN channel for benchmarking.

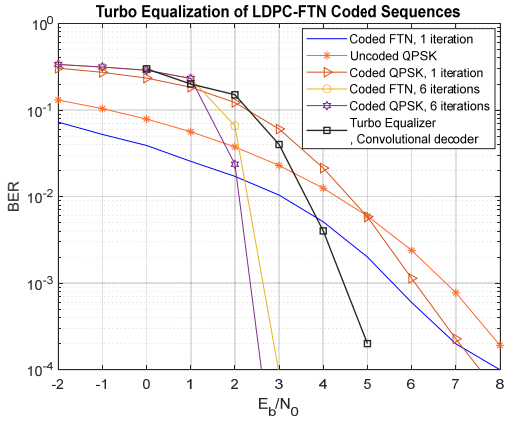

Fig. 9. BER vs E_b/N_0 (dB) for turbo equalization of coded FTN sequences with system parameters as follows: BG1 base matrix, z=32, and number of inner iterations 1 and 6. For the LDPC-coded QPSK of the same transmission rate, the LDPC decoder applies 1 & 6 inner iterations.

What is noticed from Fig. 9 is many points. First, it is clear how increasing the number of inner iterations from 1 to 6 has significantly improved the overall LDPC-FTN performance. If it is to examine the FTN curve, it becomes evident that the waterfall region has approximately a 3.5 dB enhancement. This is a more significant improvement if compared with Fig. 7 and Fig. 8. The improvement is more remarkable than when using an expansion factor of 2 because, in this case, z = 32, the density of the parity-check matrix is way less than when z = 2. Additionally, it is noticed that in the low SNR region, the curve of the 6-iterations scheme is the worst. This is because, in this region, the very low energy per channel symbol does not allow the decoder to compensate for the poor performance of the demodulator. However, as soon as we go beyond this region, particularly in the waterfall region, the added redundancy of the LDPC code starts to compensate for the fast signaling, less energy per symbol, and more errors out of the demodulator. In addition, it is noticed that the performance of binary-modulated LDPC-coded FTN with $\tau = 0.5$ is almost typical of that of the LDPC-coded QPSK transmission system, which is clearly readable from Fig. 9 for a number of inner iterations of 6. Again, this manifests the power and promising accomplishments that the faster-than-Nyquist signaling can attain. Thus, it proves the potential of FTN signaling, where with a binary modulation scheme, it is doubling the data rate at the same bandwidth, and this is achieved with a compression factor of 0.5. As smaller values of the compression factor of the FTN channel are explored in the future, we will get more spectral-efficient LDPC-coded FTN systems. By comparing the "coded FTN with 6 iterations" curve with the "turbo equalizer convolutional decoder" in Fig. 9, we notice the superiority of 5G NR LDPC code over the convolutional code over the same system setup where ~2.5 dB of SNR improvement is gained using the former scheme.

Figs. 10 and 11 generate the LDPC-coded sequences using base matrices from BG2. In Fig. 10, the expansion factor is 3, and the BER curves are attained by employing one inner iteration, six inner iterations, and uncoded QPSK over the AWGN channel, respectively.

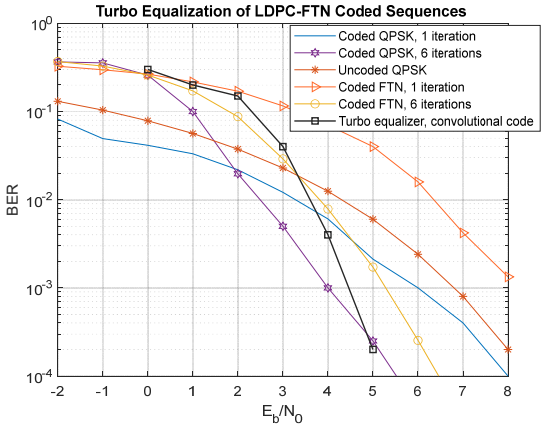

Fig. 10. BER vs E_b/N_0 (dB) for turbo equalization of coded FTN sequences with system parameters as follows: BG2 base matrix, z=3, and number of inner iterations 1 and 6. For the LDPC-coded QPSK of the same transmission rate, the LDPC decoder applies 6 inner iterations.

In comparing two LDPC systems, one employing z=2 from BG1 and the other employing z=3 from BG2, where the two expansion factors are almost the same, it is noticed from Fig. 10 that the performance of the system of z=3 from BG2 is clearly superior to that of Fig. 7 and Fig. 8. This conforms to the expectations from Eqs. (11) and (12). This is because the redundancy in BG2 base matrices is greater than that in base matrices from BG1.

Furthermore, it is shown in Fig. 10 how the low SNR region is not performing good for the 6-iterations LDPC decoding, which is due to the previously mentioned reason that the code power cannot be manifested in this region due to the extremely insufficient symbol energy. It is also noticed through all the presented figures that the performance of all systems when applying only one inner iteration for the LDPC decoder is very poor and resembles the performance of an uncoded system. This is because applying one inner iteration only at the LDPC decoder does not allow for a sufficient degree of certainty in the soft information being exchanged between the check and bit nodes on the Tanner graph of the code.

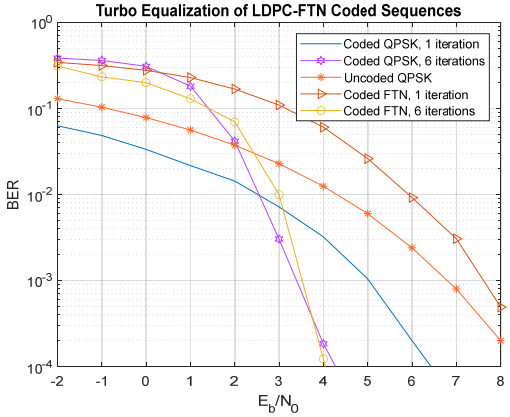

Fig. 11. BER vs E_b/N_0 (dB) for turbo equalization of coded FTN sequences with system parameters as follows: BG2 base matrix, z = 12, and number of inner iterations 1 and 6. For the LDPC-coded QPSK of the same transmission rate, the LDPC decoder applies 6 inner iterations.

In Fig. 11, another instance of performance is depicted when employing a different base matrix from BG2 but with a greater value of expansion factor of 12. It is clear from the figure that using an expansion of 12 gives better BER results when compared to those of Fig. 10, which are based on an expansion of 3.

In summary, for all the simulations, it is clear that the BER curves attained with 6 inner LDPC iterations are more reliable and consistent as compared with those of 1 inner iteration. Additionally, the performance of the considered system improves considerably as the expansion factor of the base matrix increases.

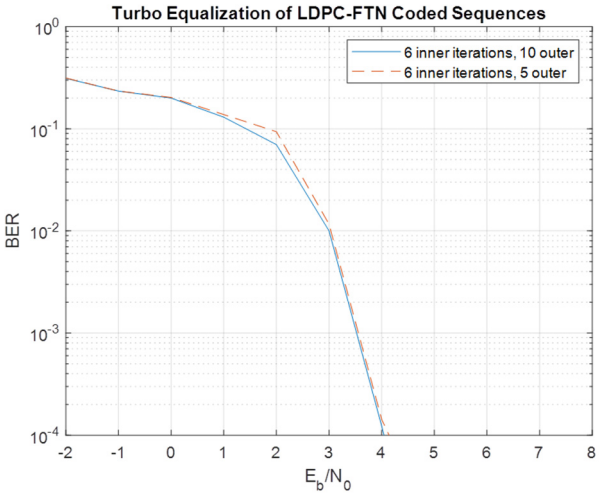

Fig. 12. BER curves vs E_b/N_0 (dB) for turbo equalization of coded FTN sequences with system parameters as follows: BG2 base matrix, z=12, and number of outer iterations 5 and 10. The number of inner iterations in both simulations is 6.

It is worth mentioning here that in all simulations we have applied 10 iterations for the outer decoding loop since there is no improvement noticed in the BER beyond this number. Whereas, BER curves worsen for (<10) outer loops. Fig. 12 shows the difference between the two BER curves attained when applying 10 and 5 outer loops, respectively. In addition, It is noticed from Fig. 12 that ~1 dB is attained at some points when moving from 5 to 10 outer iterations.

VII. Complexity and System Trade-off

It is worth mentioning here that the complexity of the turbo equalizer of FTN signals is influenced by the complexity of its two constituent block decoders, which are the inner MAP (M-BCJR) equalizer and the outer 5G LDPC belief propagation (BP) decoder. Table I provides information about the computational burden of the utilized turbo receiver.

Convergence of the inner turbo equalizer is achieved within 10 iterations, where each iteration takes ~40 seconds to run. As per the LDPC decoder, convergence is achieved within 6 iterations, and decoding times on the order of seconds per iteration are attained. So the whole processing time of the system is on the order of ~10×40s+6×10s.

TABLE I. Complexity Calculations of the Overall Detector

	Complexity	Details
M-BCJR Equalizer	~ $M \times \|\Omega\| \times N$	*M is the number of best- surviving states in the BCJR algorithm* $\|\Omega\|$ *is the modulation alphabet N is the block length.*
5G LDPC BP Decoder	~ $\mathcal{O}$ *(N+(N-K))*	*N and (N-K) ~ expansion factor (z) N is the number of bit nodes and (N-K) is the number of check nodes in the Tanner graph.*

In the context of turbo equalization for FTN signaling using 5G NR LDPC codes, several trade-offs must be considered to optimize system performance. These trade-offs involve balancing various factors to achieve the desired communication goals. Here are critical trade-offs in this context:

- The system realizes increased spectral efficiency at the cost of additional computational complexity (as the value of τ decreases, the trellis size grows bigger as the number of states increases).
- The excellent error correction performance comes at the cost of additional latency, particularly when multiple iterations are performed.
- The computationally intensive processing of the LDPC turbo equalization, the need for memory units, and, if aimed for low-latency real-time communications, all contribute to significant power consumption.

The combination of 5G LDPC codes and turbo equalization for FTN signaling is feasible and can provide robust performance in communication systems. Because it involves the turbo equalization which is effective in combating the severe ISI introduced by different channel conditions combined with the LDPC codes adopted in 5G communication systems and well-known for their excellent error-correction performance. Therefore, this combined system of turbo equalization followed by an outer LDPC decoder is feasible and can provide robust performance. However, careful consideration of computational complexity and latency, along with dealing with specialized hardware or optimized software libraries, are essential to ensure practical viability. In [32], the application of FTN in 6G communications is discussed and its value and challenges in 6G are presented. In [33–37], the authors studied the hardware design, decoding algorithm and performance analysis of FTN transceiver under multi-carrier systems. Additionally, in [38] the author studies the design and performance analysis of FTN solutions in high-speed mobile scenarios. Furthermore, FTN can be beneficially combined with other new technologies, such as deep learning, non-orthogonal multiple access (NOMA) according to [39] and [40], respectively.

VIII. Conclusions

In this article, we have applied the 5G NR LDPC codes for the turbo equalization of the FTN signaling. The performance of binary LDPC-coded FTN with τ=0.5

has been benchmarked against LDPC-coded QPSK, demonstrating similar BERs at the same data rate and bit energy consumption. Our key findings show that the proposed transmission scheme achieves superior BER performance while doubling the amount of spectral efficiency. Additionally, it is shown that increasing the number of iterations in the LDPC decoder has influenced the performance significantly.

The integration of 5G NR LDPC codes introduces a powerful error correction mechanism that is critical for mitigating the effects of the severe ISI inherent in FTN signaling. Furthermore, the regularity of the 5G NR LDPC base graphs provides an advantageous foundation for efficient decoding algorithms that can lower the intensive computational complexity for decoding FTN signals.

It has been also proved that applying the layered LDPC decoding contributes to the fast convergence of the decoding process since approximately only 6 iterations are used for good convergence. Additional contributions involve the utilization of the M-BCJR algorithm at the equalizer that allows for a handy means of controlling the complexity of the FTN receiver.

The significance of our research work lies in the fact that both the 5G NR LDPC base graphs and the FTN signaling are emerging technologies. Both schemes have the potential to accommodate the increasing demand for higher data rates in future wireless communication systems. The area of our research exploits the availability of well-structured 5G NR LDPC codes, which aligns our work with the global standards set by the 3rd generation partnership (3GPP) for the 5G NR communication systems. This ensures interoperability and compatibility with 5G networks worldwide.

IX. Future Work

The potential optimizations for our current work include exploring alternative transmission pulses other than the root raised-cosine pulses for the FTN system. The newly-explored pulses should manifest desired characteristics, such as controlled sidelobes for minimizing interference. Other optimization plans should consider the possibility of optimizing the 5G NR LDPC base matrices for the specific severe-ISI FTN channels. Additionally, the same proposed scheme will be investigated again using some of the well-known reduced complexity LDPC decoders, preferably using linear approaches for power management.

Both the short-term and long-term future research should consider the following:

- Exploring 6G technologies for handling the FTN transmission systems.
- Investigating further strategies for optimizing the performance of the 5G LDPC codes in the context of turbo equalization for FTN signaling. Explore algorithmic enhancements, parameter tuning, or novel decoding techniques to improve error correction capabilities and decoding efficiency.
- Exploring the potential benefits of combining 5G LDPC codes with other coding schemes or equalization techniques, such as hybrid approaches that leverage the strengths of different coding and equalization methods to achieve superior performance.
- Exploring techniques for reducing the number of iterations required for satisfactory convergence while maintaining high error correction performance, making the system more suitable for low-latency communication applications.
- Investigating how the proposed turbo equalization scheme can be integrated with emerging technologies, such as non-orthogonal multiple access (NOMA) to enhance the overall performance of 5G communication systems.

Conflict of Interest

The authors declare no conflict of interest.

Author Contributions

Asma A. Alqudah: Conceptualization, methodology, formal analysis, software, writing-original draft, writing-review & editing, visualization, and supervision. Khaled F. Hayajneh: Investigation, resources, data curation, writing-review & editing, visualization, and supervision. Hasan A. Aldiabat: Investigation, resources, data curation, writing-review & editing, visualization, and supervision. Hazim M. Shakhatreh: Investigation, resources, data curation, writing-review & editing, visualization, and supervision.

References

[1] R. G. Gallager, "Low density parity check codes," *Monograph*, MIT Press, 1963.

[2] D. J. C. MacKay and R. M. Neal, "Near Shannon limit performance of low-density parity-check codes," *IEEE Electron. Lett.*, vol. 32, pp. 1645–1646, 1996.

[3] D. J. C. Mackay, S. T. Wilson, and M. C. Davey, "Comparison of constructions of irregular Gallager codes," *IEEE Trans. Commun.* vol. 47, pp. 1449–1454, 1999.

[4] T. J. Richardson, M. A. Shokrollahi, and R. L. Urbanke, "Design of capacity-approaching irregular low-density parity-check codes," *IEEE Trans. Inf. Theory*, vol. 47, pp. 619–637, 2001.

[5] V. Ulkarni and K. J. Sankar, "Design of structured irregular LDPC codes from structured regular LDPC codes," in *Proc. the 2015 Third International Conference on Computer, Communication, Control and Information Technology (C3IT)*, Hooghly, India, 2015.

[6] J. E. Mazo, "Faster-than-Nyquist signaling," *Bell System Technical Journal*, vol. 54, no. 8, pp. 1451–1462, 1975.

[7] H. Nyquist, "Certain topics in telegraph transmission theory," *AIEE Transactions*, pp. 617–644, 1928.

[8] J. G. Proakis and M. Salehi, *Digital Communications*, McGraw Hill, 5th ed., 2008.

[9] F. Rusek, "Partial response and faster-than-Nyquist signaling," PhD thesis, Dept. of Electrical and Information Technology, Lund University, 2007.

[10] A. D. Liveris and C. N. Georghiades, "Exploiting faster-than-Nyquist signalling," *IEEE Transactions on Communications*, vol. 51, no. 9, pp. 1502–1511, 2003.

[11] A. Alqudah and L. Joiner, "Turbo equalization of the faster-than-Nyquist signaling using the reduced-complexity Z-MAP algorithm," *International Journal of Computer Applications & Information Technology*, vol. 9, no. 2, July 2016.

[12] W. Ryan, "Performance of high rate turbo codes on a PR4 equalized magnetic recording channel," in *Proc. IEEE Int. Conf. Communicaitons*, 1998, pp. 947–951.
[13] T. Souvignier, A. Friedman, M. Oberg, P. H. Siegel, R. E. Swanson, and J. Wolf, "Turbo decoding for PR4: Parallel versus serial concatenation," in *Proc. IEEE Int. Conf. Communications*, 1999, pp. 1638–1642.
[14] T. Duman and E. Kurtas, "Performance of turbo codes over magnetic recording channels," in *Proc. IEEE Military Communications Conf.*, 1999, pp. 806–810.
[15] E. Cerci, A. Cicek, E. Cavus, E. Bedeer, and H. Yanikomeroglu, "Coded faster-than-Nyquist signaling for short packet communications," in *Proc. 2021 IEEE 32nd Annual International Symposium on Personal, Indoor and Mobile Radio Communications*, 2021.
[16] Z. Wu and X. Huang, "A LDPC convolutional code optimization method for FTN systems," in *Proc. 3rd IEEE International Conference on Computer and Communications (ICCC)*, 2017.
[17] T. Romain, B. Bouchra, P. Charly, and B. Marie-Laure, "On coding for faster-than-Nyquist signaling," in *Proc. IEEE International Black Sea Conference on Communications and Networking (BlackSeaCom)*, Constanta, Romania, 2015.
[18] Jayawickrama, Beeshanga Abewardana, and Ying He, "Improved layered normalized min-sum algorithm for 5G NR LDPC," *IEEE Wireless Communications Letters*, vol 11, no. 9, pp. 2015-2018, 2022.
[19] R. Kingston, Michaelraj, S. Kumari, and P. Anguraj, "Certain investigations on recent advances in the design of decoding algorithms using low-density parity-check codes and its applications," *International Journal of Communication Systems* vol. 34, no. 8, 2021.
[20] H. Zhitong, K. Peng, and J. Song, "Multi-layer progressive tree-structured edge growth algorithm for nested lifting design of 5G-NR-Like LDPC codes," *IEEE Communications Letters*, vol. 26, no. 12, pp. 2836-2840, 2022.
[21] R. Kingston, and P. Anguraj, "A comparative review of recent advances in decoding algorithms for Low-Density Parity-Check (LDPC) codes and their applications," *Archives of Computational Methods in Engineering*, vol. 28, no. 4, pp. 2225-2251, 2021.
[22] S. Khittiwitchayakul, W. Phakphisut and P. Supnithi, "Sliding-window processing of turbo equalization for partial response channels," in *Proc. 26th International Conference on Telecommunications (ICT)*, Hanoi, Vietnam, 2019, pp. 182-186, doi: 10.1109/ICT.2019.8798835.
[23] N. Zhang, Z. Qin, Y. Li, L. Xing, Q. Lu, and X. Liu, "Quantized turbo equalization for nonbinary LDPC coded partial-response channels," *International Journal of Future Computer and Communication*, vol. 10, no. 1, 2021.
[24] A-M Cuc, F. Lucian, A-M Grava, and C. Grava, "Iterative equalization and decoding over additive white Gaussian noise channel with ISI using low-density parity-check codes," *App. Sci*, vol 13, no. 22, pp. 12294, 2023.
[25] J. B. Anderson and A. Prlja, "Turbo equalization and an M-BCJR algorithm for strongly narrowband intersymbol interference," *Information Theory and Its Applications (ISITA)*, pp. 261–266, 2010.
[26] A. D. Liveris and C. N. Georghiades, "Exploiting faster-than-Nyquist signaling," *IEEE Transactions on Communications*, vol. 51, no. 9, pp. 1502–1511, 2003.
[27] M. E. Hefnawy and H. Taoka, "Overview of faster-than-Nyquist for future mobile communication systems," in *Proc. Vehicular Technology Conference (VTC Spring)*, 2013, pp. 1–5.
[28] Y. J. D. Kim and J. Bajcsy, "On spectrum broadening of pre-coded faster-than-Nyquist signaling," in *Proc. Vehicular Technology Conference*, 2010, pp. 1–5.
[29] Y. Yoo and G. Cho, "Asymptotic optimality of binary faster-than-Nyquist signaling," *IEEE Communications Letters*, vol. 14, no. 9, pp. 788–790, 2010.
[30] M. McGuire and M. Sima, "Discrete time faster-than-Nyquist signaling," in *Proc. IEEE Global Telecommunications Conference*, 2010, pp. 1–5.
[31] 3GPP TS 38.212. Technical Specification Group Radio Access Network; NR; Multiplexing and channel coding (release 16). [Online]. Available: https://portal.3gpp.org/desktopmodules/
[32] X. Su, S. Wang, Y. Hongwen, J. Jing, and Q. Wang, "Super Nyquist transmission technology: Application value and challenges for 6G." *Telecommunications Science*, vol. 37, no. 9, pp. 38-47, 2021.
[33] D. Dasalukunte, F. Rusek, J. B. Anderson *et al*., "Design and implementation of iterative decoder for faster-than-Nyquist signaling multicarrier systems," in *Proc. 2011 IEEE Computer Society Annual Symposium on VLSI, Piscataway: IEEE Press*, 2011, pp. 359-360.
[34] D. Dasalukunte, F. Rusek, and V. Owall, "Multicarrier faster-than-Nyquist transceivers: hardware architecture and performance analysis," *IEEE Transactions on Circuits and Systems I: Regular papers*, vol. 58, no. 4, pp. 827-838, 2011.
[35] D. Dasalukunte, F. Rusek, and V. Öwall, "An iterative decoder for multicarrier faster-than-Nyquist signaling systems," in *Proc. 2010 IEEE International Conference on Communications. Piscataway: IEEE Press*, 2010, pp. 1-5.
[36] D. Dasalukunte, F. Rusek, and V. Öwall, "Improved memory architecture for multicarrier faster-than-Nyquist iterative decoder," in *Proc. 2011 IEEE Computer Society Annual Symposium on VLSI Piscataway: IEEE Press*, 2011 pp. 296-300.
[37] D. Dasalukunte, F. Rusek, and V. Öwall, "An 0.8-mm(2)9.6-mW iterative decoder for faster-than-Nyquist and orthogonal signaling multicarrier systems in 65-nm CMOS," *IEEE Journal of Solid-State Circuits*, vol. 48, no. 7, pp. 1680-1688, 2013.
[38] Z. Lei, "Analysis of super-Nyquist and time-domain overlap multiplexing transmission performance in high mobility scenarios," *Chengdu: Southwest Jiaotong University*, 2015.
[39] P. Y. Song, F. K. Gong, Q. Li *et al.*, "Receiver design for faster-than-Nyquist signaling: deep-learning-based architectures," *IEEE Access*, vol. 8, pp. 68866-68873, 2020.
[40] W. J. Yuan, N. Wu, Q. H. Guo *et al.*, "Iterative joint channel estimation, user activity tracking, and data detection for FTN-NOMA systems supporting random access," *IEEE Transactions on Communications*, vol. 68, no. 5, pp. 2963-2977, 2020.